

# Role of chirality in peptide-induced formation of cholesterol-rich domains

Richard M. EPAND\*<sup>1</sup>, Scott D. RYCHNOVSKY†, Jitendra D. BELANI† and Raquel F. EPAND\*

\*Department of Biochemistry, McMaster University, 1200 Main Street West, Hamilton, Ontario, Canada L8N 3Z5, and †Department of Chemistry, 516 Rowland Hall, University of California, Irvine, CA 92697-2025, U.S.A.

The chiral specificity of the interactions of peptides that induce the formation of cholesterol-rich domains has not been extensively investigated. Both the peptide and most lipids are chiral, so there is a possibility that interactions between peptide and lipid could require chiral recognition. On the other hand, in our models with small peptides, the extent of folding of the peptide to form a specific binding pocket is limited. We have determined that replacing cholesterol with its enantiomer, *ent*-cholesterol, alters the modulation of lipid organization by peptides. The phase-transition properties of SOPC (1-stearoyl-2-oleoylphosphatidylcholine):cholesterol [in a 6:4 ratio with 0.2 mol % PtdIns(4,5)*P*<sub>2</sub>] are not significantly altered when *ent*-cholesterol replaces cholesterol. However, in the presence of 10 mol % of a 19-amino-acid, N-terminally myristoylated fragment (myristoyl-GGKLSKK-KKGYNVNDEKAK-amide) of the protein NAP-22 (neuronal axonal membrane protein), the lipid mixture containing cholesterol undergoes separation into cholesterol-rich and cholesterol-depleted domains. This does not occur when *ent*-cholesterol

replaces cholesterol. In another example, when *N*-acetyl-Leu-Trp-Tyr-Ile-Lys-amide (*N*-acetyl-LWYIK-amide) is added to SOPC:cholesterol (7:3 ratio), there is a marked increase in the transition enthalpy of the phospholipid, indicating separation of a cholesterol-depleted domain of SOPC. This phenomenon completely disappears when *ent*-cholesterol replaces cholesterol. The all-*D*-isomer of *N*-acetyl-LWYIK-amide also induces the formation of cholesterol-rich domains with natural cholesterol, but does so to a lesser extent with *ent*-cholesterol. Thus specific peptide chirality is not required for interaction with cholesterol-containing membranes. However, a specific chirality of membrane lipids is required for peptide-induced formation of cholesterol-rich domains.

**Key words:** cholesterol, cholesterol enantiomer, chirality, CRAC motif, membrane domain, neuronal axonal membrane protein (NAP-22).

## INTRODUCTION

It is now generally accepted that the molecular components of biological membranes are not uniformly distributed, but are enriched in specific regions or domains. Some of these domains are enriched in cholesterol and sphingomyelin, and have been termed 'rafts' [1]. In addition to interactions with lipids, proteins also affect the distribution of cholesterol in membranes [2]. Two examples of this are NAP-22 {neuronal axonal membrane protein [also referred to as brain acid soluble protein 1 (BASP1 protein)], a 22 kDa myristoylated protein} [3] and the segment LWYIK (Leu-Trp-Tyr-Ile-Lys) from the gp41 protein of HIV [4]. NAP-22 is a 22 kDa protein found in neurons that is important for neuronal sprouting and plasticity [5]. In addition to the intact 22 kDa protein, significant amounts of N-terminal myristoylated fragments of this protein are also found in many tissues [6]. Myristoylated proteins are commonly found in cholesterol-rich domains in membranes [7,8]. A 19-amino-acid N-terminal peptide of NAP-22 (NAP-22 peptide; Figure 1), which is found physiologically, sequesters PtdIns(4,5)*P*<sub>2</sub> into domains in a cholesterol-dependent manner [9]. The segment LWYIK is part of the tryptophan-rich region of gp41 that is adjacent to the trans-membrane helix. This region of the protein is important for both infectivity and for sequestering into raft domains [10–12].

Both the so-called CRAC [13] motif as well as protein acylation are relatively non-specific mechanisms for interaction of proteins with membranes, since they do not involve a conformationally specific rigid binding site. Nevertheless, these two features are sufficient to determine preferential interaction with cholesterol in membrane bilayers. In the present study we determine the role

of cholesterol chirality on the interaction of these peptides with membranes. For this purpose, we have used natural cholesterol and its enantiomer, *ent*-cholesterol, in which each of the chiral centres of the natural form was inverted (Figure 1). Our study employed both DSC (differential scanning calorimetry) and <sup>1</sup>H NOESY (nuclear Overhauser enhancement spectroscopy) MAS (magic angle spinning)-NMR. DSC allows us to monitor the extent to which cholesterol has been depleted from a domain in the membrane by measuring the enthalpy and co-operativity of the chain melting transition of the phospholipid. It is well known that cholesterol broadens phospholipid-phase transitions and lowers the gel-to-liquid/crystalline-phase transition enthalpy. As a result of peptide-induced phase separation of lipid components, the presence of cholesterol-depleted domains will be revealed by an increase in the enthalpy and co-operativity of this transition [2]. The NOESY MAS/NMR measurements provide an estimate of the groups which come into close contact with the aromatic groups of the peptide [14]. Both methods allow the use of lipids without fluorescent probes, and are able to detect the presence of domains smaller than those required for detection by fluorescence microscopy.

## EXPERIMENTAL

### Materials

A synthetic lipopeptide (myristoyl-GGKLSKKKKKGYNVNDEKAK-amide, corresponding to the 19 N-terminal residues of NAP-22), was purchased from BioSource International (Hopkinton, MA, U.S.A.). The peptide *N*-acetyl-LWYIK-amide

Abbreviations used: 2D, two-dimensional; (SO/PO)PC, (1-stearoyl-2-oleoyl/1-palmitoyl-2-oleoyl)phosphatidylcholine; DPPC, dipalmitoyl-PC; DSC, differential scanning calorimetry; MAS, magic angle spinning; NAP-22, neuronal axonal membrane protein; NOESY, nuclear Overhauser enhancement spectroscopy.

<sup>1</sup> To whom correspondence should be addressed (email epand@mcmaster.ca).

**Nap-22 peptide:**  
Myristoyl-GGKLSKKKKGYNVNDEKAK-amide

**HIV gp-41 peptide:**  
N-Acetyl-LWYIK-amide

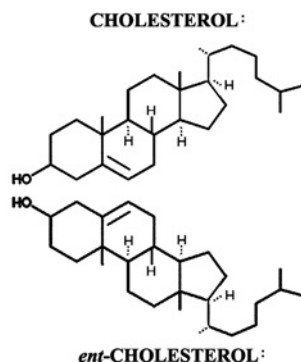


**Figure 1** Structures of peptides, cholesterol and *ent*-cholesterol

and its all-D-amino-acid isomer were synthesized by SynPep Corp. (Dublin, CA, U.S.A.) and purified by HPLC. *ent*-Cholesterol was synthesized and characterized as described previously [15]. Cholesterol and phospholipids, including PtdIns(4,5) $P_2$ , purified from porcine brain, were purchased from Avanti Polar Lipids (Alabaster, AL, U.S.A.).

#### Preparation of samples for DSC and NMR experiments

Lipid components were co-dissolved in chloroform/methanol (2:1, v/v). For samples containing peptide, an aliquot of a solution of the peptide in methanol was added to the lipid solution in chloroform/methanol. The amount of peptide used was monitored by the absorbance at 280 nm using an absorption coefficient calculated from the amino acid composition [16]. The solvent was rapidly evaporated at 30 °C under a stream of nitrogen with constant rotation of a test tube to avoid separation of lipid components [17], and to deposit a uniform film of lipid over the bottom third of the tube. Last traces of solvent were removed by placing the tube under high vacuum for at least 2 h. The lipid film was then hydrated with 20 mM Pipes containing 1 mM EDTA and 150 mM NaCl with 0.002 %  $\text{NaN}_3$ , pH 7.4, and suspended by intermittent vortex-mixing and heating to 50 °C over a period of 2 min under argon. Samples used for NMR analysis were hydrated with the same buffer made in  $^2\text{H}_2\text{O}$  and adjusted to a pH meter reading of 7.0 ( $p^2\text{H}_2 = 7.4$ ), and incubated for at least 24 h at 4 °C to allow conversion of any anhydrous cholesterol or *ent*-cholesterol crystals into the monohydrate form. For NMR measurements, the samples were first spun in an Eppendorf centrifuge at room temperature. The resulting hydrated pellet was transferred to a 4 mm zirconia rotor with the 12  $\mu\text{l}$  Kel-F insert, attempting to pack the maximal amount of lipid into the rotor while maintaining its wetness.

#### DSC experiments

Measurements were made using a Nano Differential Scanning Calorimeter (Calorimetry Sciences Corp., American Fork, UT, U.S.A.). A lipid concentration of 2.5 mg/ml was used either with or without the addition of between 5 and 15 mol % peptide. The scan rate was 2 °C/min, and there was a delay of 5 min between sequential scans in a series to allow for thermal equilibration. Each set of scans presented was repeated at least twice with two

independent preparations giving similar results. The features of the design of this instrument have been described previously [18]. DSC curves were analysed by using the fitting program DA-2, provided by Microcal Inc. (Northampton, MA, U.S.A.) and plotted with Origin, version 5.0.

#### $^1\text{H}$ NOESY MAS-NMR

High resolution MAS spectra were acquired using a spinning speed of 5.5 kHz in a Bruker AV 500 NMR spectrometer. The 12  $\mu\text{l}$  insert of the rotor was packed with as much of the centrifuged pellet as possible. The probe temperature was  $24 \pm 1$  °C. The 2D (two-dimensional)-NOESY spectra were obtained using delay times of 50 and 300 ms. Resonances were assigned based on reports of PC (phosphatidylcholine) [19], cholesterol [20] and amino acid residues [21].

#### CD experiments

CD spectra were recorded with an AVIV Model 215 Circular Dichroism Spectrometer (Proterion Corp., Piscataway, N.J., U.S.A.). The sample was contained in a 2 mm quartz cell that was maintained at 25 °C in a thermostat-controlled cell holder. CD data were expressed as mean residue ellipticities. All CD measurements were performed in 10 mM sodium phosphate/0.14 M NaCl, pH 7.4. For peptide alone, solutions were made from methanol and diluted into buffer to a concentration of 150  $\mu\text{M}$ . Lipid films containing peptide were made by mixing all components in chloroform/methanol (2:1, v/v) and dried under nitrogen and vacuum. Films were hydrated with phosphate buffer by vortex-mixing, and were then sonicated to clarity before measuring the CD. The lipid concentration was 500  $\mu\text{M}$ .

## RESULTS

#### DSC experiments

We compared the effect of the myristoylated NAP-22 peptide on the phase transitions of a mixture of SO(1-stearoyl-2-oleoyl)PC/cholesterol/PtdIns(4,5) $P_2$  (300/200/1, by vol.) with the corresponding mixture in which cholesterol was replaced by *ent*-cholesterol. For each sample, six consecutive scans were run, three heating scans and three cooling scans at a scan rate of 2 °C/min. Sequential heating and cooling scans were reproducible and exhibited a transition in the region 0–10 °C, corresponding to the chain melting transition of SOPC. The transitions are better resolved in cooling than in heating scans, since in some cases the heating scans, initiated at 0 °C, had not reached a steady-state baseline at the temperatures of the transition. Since data are calculated as the difference between a sample run and a baseline (buffer vs. buffer) run, and both are steeply sloping before reaching the steady state, data near the initiation of the scan can be distorted, especially if the excess heat capacity is small, as shown in Figure 2 (bottom right panel). In the absence of peptide, the two lipid mixtures exhibited very similar DSC curves (Figure 2), but upon addition of 10 mol % of the NAP-22 peptide, the mixture with cholesterol exhibited a large increase in the enthalpy of the chain melting transition, suggesting that, at least in this temperature range, there was an area in the membrane that was depleted of cholesterol. The enthalpy for the transition, observed at 1.6 °C in the cooling scan for the mixture of SOPC/cholesterol/PtdIns(4,5) $P_2$ /NAP-22 peptide, is 0.85 kcal/mol SOPC (1 cal  $\equiv$  4.184 J). This is dramatically different from the results with the mixture in which *ent*-cholesterol replaces cholesterol in the presence of the peptide, for which the chain melting transition has essentially completely disappeared (Figure 2). We

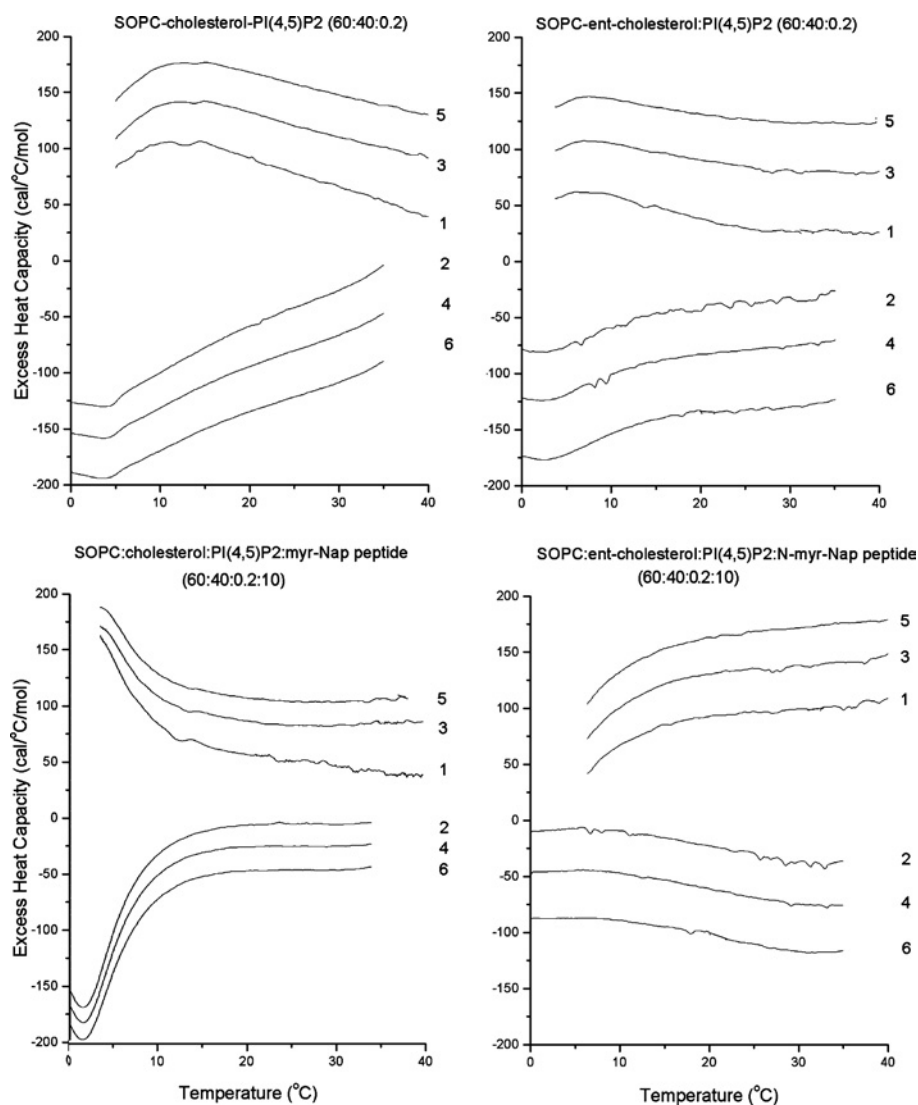


**Figure 2** DSC of SOPC:cholesterol (6:4) or SOPC:*ent*-cholesterol (6:4) with 0.2 mol % PtdIns(4,5) $P_2$  with or without 10 mol % NAP-22 peptide

The scan rate was 2K/min, and the lipid concentration was 2.5 mg/ml in 20 mM Pipes containing 1 mM EDTA and 150 mM NaCl supplemented with 0.002% Na $N_3$ , pH 7.4. Sequential heating and cooling scans was performed between 0 and 50 °C. Numbers are the order in which the scans were carried out, with scans 1, 3 and 5 being heating scans, each of which was followed by one of the cooling scans 2, 4 or 6. Scans are displaced along the  $y$ -axis for clarity of presentation. myr, myristoylated; PI, PtdIns; 1 cal = 4.184 J.

also compared the DSC of this lipid mixture with either cholesterol or *ent*-cholesterol in the presence of lower concentrations of NAP-22 peptide (2.5 and 5 mol %). In all cases, the observable transition enthalpy of the SOPC chain melting was greater in the mixtures with cholesterol than in those with *ent*-cholesterol. For mixtures with 2.5 mol % NAP-22 peptide, the chain melting transition was discernable with both the cholesterol and *ent*-cholesterol-containing samples, but was larger in the case of cholesterol (results not shown). With the lipid mixture of SOPC/cholesterol/PtdIns(4,5) $P_2$  in the absence of peptide, the transition is too broad to estimate the enthalpy, but it is clearly markedly lower and similar to the mixture in which *ent*-cholesterol replaces cholesterol in the absence of peptide (Figure 2).

We also determined the effect of *N*-acetyl-LWYIK-amide on mixtures of SOPC/cholesterol (7:3) compared with SOPC/*ent*-cholesterol (7:3; Figure 3). Addition of *N*-acetyl-LWYIK-amide to the mixture with cholesterol increases the transition enthalpy in this mixture to a greater extent than when *ent*-cholesterol re-

places the natural isomer of cholesterol (Figure 3). The effect of cholesterol chirality is not as dramatic in this case as in the example with the NAP-22 peptide. Nevertheless, there is a selective increase in the chain melting transition induced by *N*-acetyl-LWYIK-amide in the cholesterol-containing membrane, but not in the one with *ent*-cholesterol at both a 7:3 and a 6:4 SOPC:sterol ratio (Table 1). All three components in the mixture of *N*-acetyl-LWYIK-amide with SOPC and cholesterol are chiral. We have also determined how the chirality of the peptide affects the phase behaviour of the mixture. *N*-Acetyl-lwyik-amide (the all-D isomer, as denoted by the lowercase letters for the amino acids) has similar effects to those of the L-isomer of the peptide on the phase transition of mixtures of SOPC with cholesterol, and it also has a smaller effect on mixtures with *ent*-cholesterol (Table 1).

The range of peptide-to-lipid ratios used is limited, because when the peptide is below 5 % of the lipid, little effect is observed and the use of more than 15 % peptide risks having non-specific

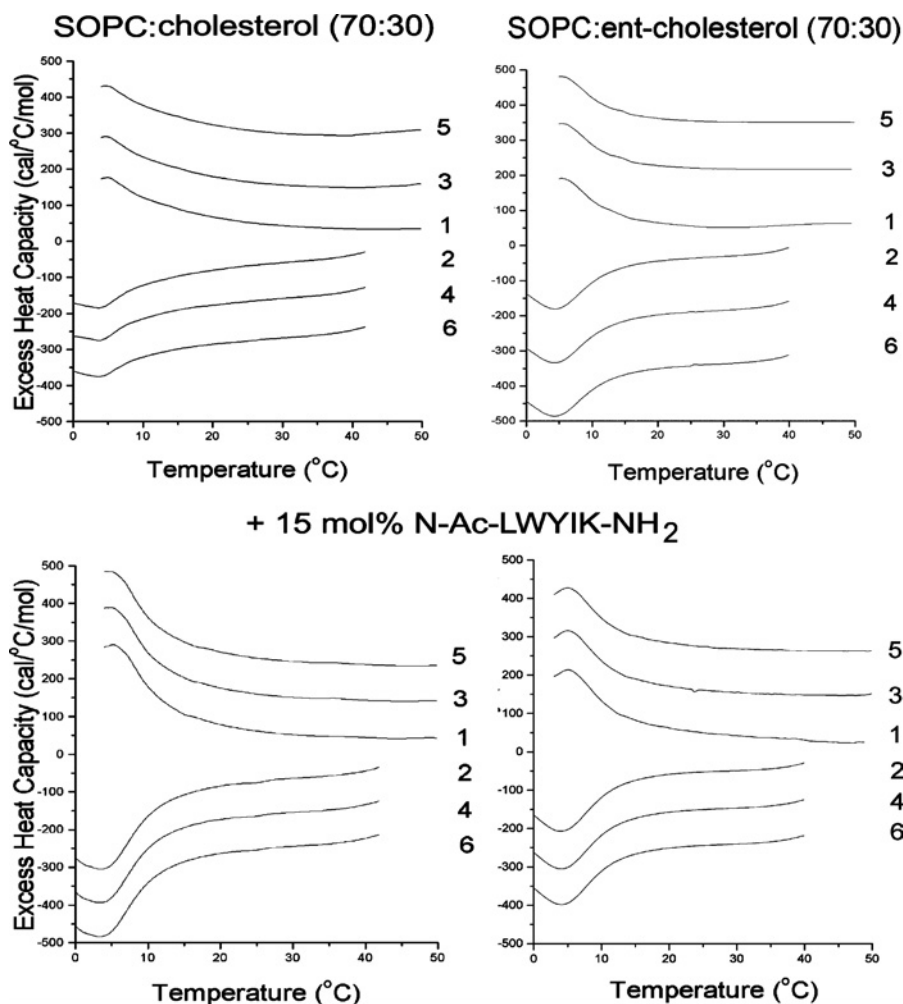


**Figure 3** DSC of SOPC:cholesterol (7:3) (left panels) or SOPC:*ent*-cholesterol (7:3) (right panels) with or without 15 mol% *N*-acetyl-LWYIK-amide

The scan rate was 2K/min and the lipid concentration was 2.5 mg/ml in 20 mM Pipes containing 1 mM EDTA and 150 mM NaCl supplemented with 0.002% NaN<sub>3</sub>, pH 7.4. Sequential heating and cooling scans between 0 and 50 °C are shown. Numbers are the order in which the scans were carried out, with scans 1, 3 and 5 being heating scans, each of which was followed by one of the cooling scans 2, 4 or 6. Scans were displaced along the *y*-axis for clarity of presentation. Ac, acetyl; 1 cal = 4.184 J.

**Table 1** DSC data showing the chain melting transition

*T<sub>m</sub>*, transition temperature;  $\Delta H$ , calorimetric enthalpy (1 kcal = 4.184 kJ). The all-*D* isomer of the peptide is indicated by the lowercase letters (lwyik; LWYIK refers to the all-*L* isomer of the peptide).

Sample composition		Cholesterol		<i>ent</i> -Cholesterol	
SOPC:sterol (molar ratio)	Peptide (all <i>N</i> -acetyl amides)	<i>T<sub>m</sub></i> (°C)	$\Delta H$ (kcal/mol)	<i>T<sub>m</sub></i> (°C)	$\Delta H$ (kcal/mol)
7:3	None	3.9	0.52	4.8	0.54
7:3	10% LWYIK	4.0	1.1	4.5	0.57
7:3	15% LWYIK	3.6	1.2	4.7	0.62
7:3	10% lwyik	4.2	1.0	4.1	0.80
7:3	15% lwyik	4.1	1.3	3.9	0.85
6:4	None	4.7	0.1	4.2	0.15
6:4	10% LWYIK	4.8	0.3	3.9	0.35
6:4	15% LWYIK	4.0	0.5	4.5	0.35
6:4	10% lwyik	4.8	0.4	1.5	0.16
6:4	15% lwyik	4.9	0.6	3.7	0.29

effects and disruption of the bilayer. However, within this limited range of peptide-to-lipid ratios, the increase in the observed enthalpy of the chain melting transition of SOPC is approximately

proportional to the molar fraction of peptide (Table 1, and results not shown). This suggests that oligomerization of the peptide in the membrane is not required for the redistribution of cholesterol, since that would have resulted in a co-operative effect.

### <sup>1</sup>H NOESY MAS-NMR

The only resonances of the peptide that are clearly resolved are those of the aromatic protons. In Figure 4 we present slices of the 2D-NOESY spectrum at the chemical shift of these resolved resonances of the peptide, and we assume that the observed cross-peaks are a result of dipolar interactions between the aromatic protons of the peptide and the aliphatic protons of the lipid. This is because the lipid is in approx. 10-fold molar excess, and many of the lipid resonances represent several protons. It should be noted, however, that even if some of the cross-peaks corresponded to nuclear Overhauser effect interactions within the peptide, the comparison of the spectra for samples with cholesterol and those with *ent*-cholesterol would allow one to conclude whether the chirality of the sterol affected the molecular arrangement within the peptide-lipid complex.

The slices of the 2D-NOESY spectra at the resonances of the two aromatic protons for a mixture of 10 mol % of the NAP-22

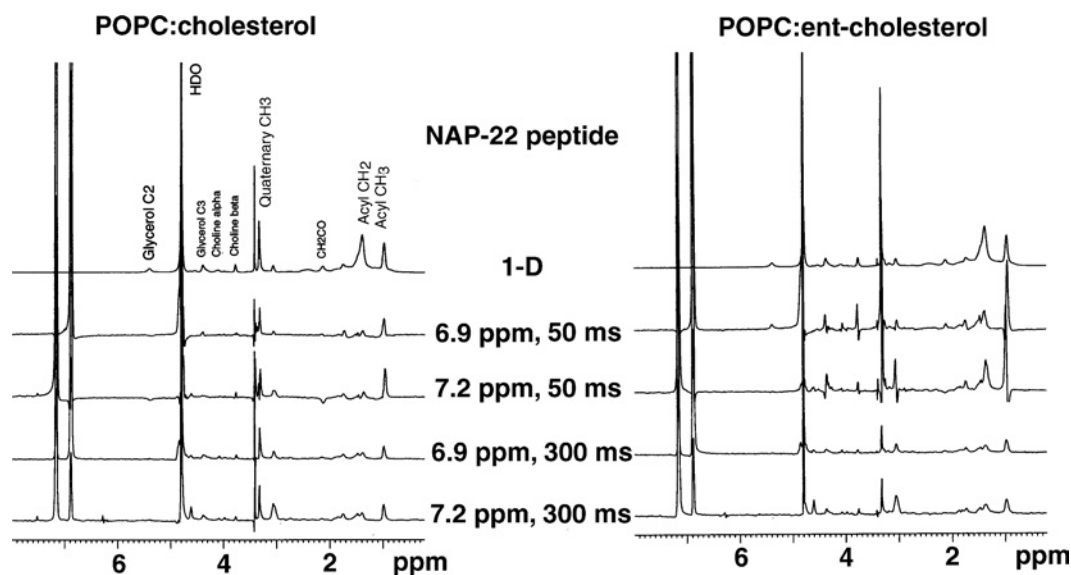


**Figure 4** One-dimensional slices from the MAS  $^1\text{H}$  NOESY spectrum at the chemical shifts of the aromatic protons using mixing times of 50 and 300 ms

Spectra are taken from samples of POPC:cholesterol (1:1) or POPC:*ent*-cholesterol (1:1), each containing 10 mol % of the NAP-22 peptide.

peptide and an equimolar mixture of PO (1-palmitoyl-2-oleoyl)PC and cholesterol or POPC and *ent*-cholesterol are shown using mixing times of 50 and 300 ms (Figure 4). The resonances at 7.2 and 6.9 p.p.m. are from the tyrosine-ring protons, with the resonance at 6.9 p.p.m. corresponding to the position closer to the tyrosine hydroxy group. Because of their close physical proximity, these two positions show strong dipolar interactions between them. The strong resonance at 4.8 p.p.m. is from residual protons in  $^2\text{H}_2\text{O}$ . The slices for the sample with cholesterol are qualitatively similar to that of the sample with *ent*-cholesterol, indicating a similar depth of penetration of the peptide in the two cases. Nevertheless, the slices are not identical, demonstrating a detectable difference in the interaction of the peptide with POPC, depending on whether cholesterol or *ent*-cholesterol is present. In particular, the sample with *ent*-cholesterol shows cross-peaks for the 50 ms spectra at 4.3 and 3.7 p.p.m., corresponding to the  $\alpha$  and  $\beta$  choline protons respectively. There are also peaks in the 6.9 p.p.m. slice using the 50 ms mixing time at 4.1 and 5.3 p.p.m., corresponding to the protons on C-1 and C-2 of glycerol. These cross-peaks are either absent or almost undetectable for the corresponding slices of the sample with cholesterol.

The differences in the NOESY slices are more evident when comparing the slices from samples of *N*-acetyl-LWYIK-amide in POPC:cholesterol compared with POPC:*ent*-cholesterol (Figure 5). In particular, the sign of the cross-peaks is inverted for the slices from the spectra taken with a 300 ms mixing time of the sample with *ent*-cholesterol, except for the slice at 7.6 p.p.m., which remains positive. The sign of the lipid cross-peaks for the other slices with *ent*-cholesterol at 300 ms are opposite to that of the aromatic resonance appearing below 6 p.p.m. The cross-peaks for the other NOESY slices all remain positive (Figure 5). This is indicative of a difference in motional properties within the membrane between the sample with cholesterol and that with *ent*-cholesterol. In addition, for the slices from the NOESY spectra with 50 ms mixing times, the magnitude of the terminal methyl group cross-peak at 0.95 p.p.m. relative to that of the 1.35 p.p.m. cross-peak for the methylene resonances is larger for the sample with *ent*-cholesterol than that for the samples with

cholesterol. With the 50 ms spectra, the cross-peak of the  $\text{CH}_2\text{CCO}$  protons at 1.7 p.p.m. is larger for the sample with cholesterol compared with that with *ent*-cholesterol (Figure 5).

#### CD spectroscopy

The NOESY cross-peaks between the aromatic protons of the peptide and protons of the lipid represent transient interactions of a dynamic structure. The dynamic nature of membrane structures is shown, for example, by neutron diffraction studies [22], as well as by NMR and modelling studies [23,24]. The CD spectrum of *N*-acetyl-LWYIK-amide does not indicate a high degree of order in the conformation of the peptide (Figure 6). Furthermore, there is no large change in the presence of lipid, and lipid mixtures with either cholesterol or *ent*-cholesterol behave similarly. This result is expected for a small pentapeptide. A quantitative interpretation of the spectra is complicated by the presence of aromatic groups that can contribute to the far-UV region of the CD spectrum, as well as possible light-scattering artifacts in the presence of lipid. This peptide would not be expected to penetrate deeply into the bilayer, as is confirmed by the small Stokes shift observed in the tryptophan fluorescence emission caused by the presence of lipid [4]. In addition, the changes observed in tryptophan emission in the presence of sonicated unilamellar vesicles of SOPC containing cholesterol were the same as when the cholesterol was replaced by *ent*-cholesterol (results not shown). The NAP-22 peptide is longer, and the CD spectrum for this lipopeptide in buffer is more typical of a random coil (Figure 6). There is a relatively small change in the presence of lipid and as with the *N*-acetyl-LWYIK-amide, the change is the same with either of the two cholesterol enantiomers. It is likely that some of the observed decrease is a consequence of light-scattering artifacts that are known to reduce the magnitude of the spectra. The polar nature of the peptide portion of NAP-22 peptide, as well as the several charged residues, would prevent it from inserting deeply in the membrane.

The CD results confirm that neither peptide forms structures with a high degree of order in the presence of lipid, and that the conformational properties of the peptides are similar in membranes with either cholesterol or *ent*-cholesterol.

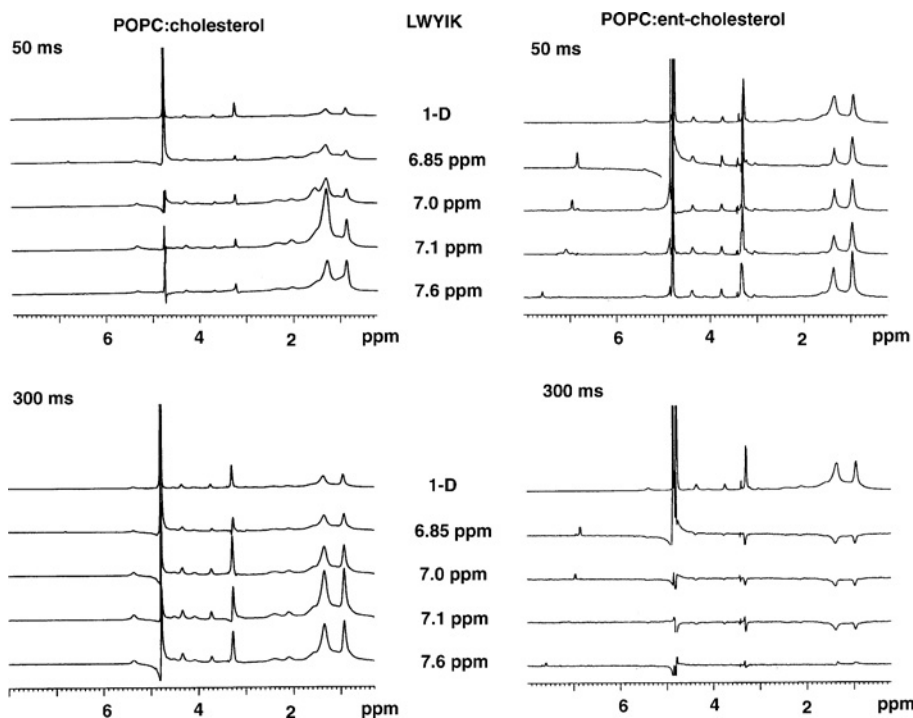


**Figure 5** One-dimensional slices from the MAS  $^1\text{H}$  NOESY spectrum at the chemical shifts of the aromatic protons using mixing times of 50 and 300 ms

Spectra are taken from samples of POPC:cholesterol (1:1) or POPC:*ent*-cholesterol (1:1), each containing 10 mol % of *N*-acetyl-LWYIK-amide.

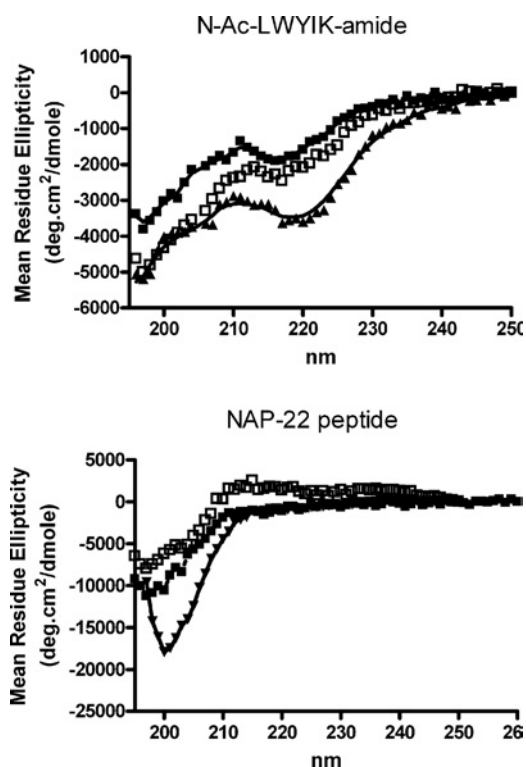


**Figure 6** CD spectra of 150  $\mu\text{M}$  *N*-acetyl-LWYIK-amide (top panel) or 150  $\mu\text{M}$  NAP-22 peptide (bottom panel)

CD spectra were run of samples in a 1 mm cell at 25 °C; the buffer comprised 10 mM sodium phosphate/140 mM NaCl. Shown are traces of peptide in buffer alone ( $\blacktriangle$ ), or with the addition of 500  $\mu\text{M}$  sonicated unilamellar vesicles of SOPC:cholesterol (1:1;  $\square$ ) or SOPC:*ent*-cholesterol (1:1;  $\blacksquare$ ).

## DISCUSSION

The relationship of the chirality of lipids and interactions with cholesterol has been studied. Several papers have shown that the two enantiomers of DPPC (dipalmitoyl-PC) interact indistinguishably with cholesterol. However, PC has only one chiral centre at the C-2 position of the glycerol moiety. In comparison, *ent*-cholesterol differs at several chiral centres from cholesterol. Nevertheless, the two enantiomers of cholesterol appear to interact identically with DPPC [25], but for certain molar ratios of egg sphingomyelin and cholesterol, differences between mixtures with cholesterol and *ent*-cholesterol had been found using monolayers [25,26]. However, more recent work has questioned this finding [27]. *ent*-Cholesterol is an enantiomer of cholesterol, i.e. the exact mirror image, rather than being a diastereoisomer that differs in configuration at only some of the chiral centres. Therefore pure cholesterol and *ent*-cholesterol should have identical physical and chemical properties (except for optical rotation). The two compounds, however, may differ in their interaction with other chiral molecules, such as phospholipids or chiral peptides. It has been concluded that there is no enantioselectivity in sterol–lipid interactions [28]. This is in general agreement with the observations we report in the present paper.

Studies with *Caenorhabditis elegans*, a cholesterol auxotroph, has shown that *ent*-cholesterol cannot replace cholesterol and maintain viability of the organism, causing lethality in the second generation [29]. This suggests that biological systems can be sensitive to the chirality of cholesterol. The enzyme cholesterol oxidase that binds specifically to cholesterol exhibits specificity for the chirality of the sterol [27]. However, other proteins, such as cholesterol antibodies [30] or sarcoplasmic/endoplasmic reticulum  $\text{Ca}^{2+}$ -ATPase-2b [31], do not discriminate between the two cholesterol enantiomers. With lytic peptides, some are not sensitive to the chirality of cholesterol, such as streptolysin, whereas

others exhibit a large effect of cholesterol chirality, having only a small effect with *ent*-cholesterol, such as *Vibrio cholerae* cytolysin [32]. *ent*-Cholesterol suppresses the antifungal activity of amphotericin to a lesser extent than cholesterol [33]. Hence there can be a variety of effects of cholesterol chirality on protein activity. Not surprisingly, proteins that have a specific binding site for cholesterol exhibit chiral specificity, whereas those whose activity is modulated by the effects of cholesterol on membrane physical properties exhibit the same effect with both cholesterol and *ent*-cholesterol. There are also intermediate cases showing small effects of cholesterol chirality.

There is limited information as to whether the chirality of cholesterol will affect the sequestering of proteins into cholesterol-rich domains in membranes. A protein thought to be located in raft domains, the P-glycoprotein, is not affected by partial replacement of cellular cholesterol with *ent*-cholesterol [34]. However, the cell membrane is a complex system in which protein–protein interactions can also play a role. In addition, depletion of cellular cholesterol by methyl cyclodextrin is only partial, indicating that cholesterol can never be fully replaced in biological membranes with its enantiomer. We have evaluated two simple examples that represent motifs by which proteins are incorporated into cholesterol-rich domains. One is the NAP-22 peptide, a lipidated peptide that sequesters into raft domains. The other is *N*-acetyl-LWYIK-amide, which has an amino acid sequence corresponding to a CRAC motif. In both cases, the peptide preferentially associates with cholesterol-rich regions of the membrane through relatively non-specific interactions, yet exhibits chiral specificity. This is most clearly seen with the DSC results of the NAP-22 peptide (Figure 2). In the absence of cholesterol, pure SOPC exhibits a phase transition with an enthalpy of 4 kcal/mol at 6 °C [4]. The enthalpy of the transition is markedly suppressed in the lipid mixture containing 40 mol % cholesterol and 0.2 mol % PtdIns(4,5) $P_2$  in the absence of peptide, and is also broadened and shifted to slightly lower temperature (Figure 2, upper left-hand panel). Replacing cholesterol with its enantiomer, *ent*-cholesterol, has almost no effect on the transition properties of this lipid mixture (Figure 2, upper right-hand panel). However, the enthalpy and co-operativity ('sharpness') of this transition dramatically increases when the NAP-22 peptide is added to this same lipid mixture (Figure 2, lower left-hand panel). This change is in marked contrast with what is observed when peptide is added to the lipid mixture in which *ent*-cholesterol replaces cholesterol. In this case, the cooling curves (scans 2, 4 and 6) show the complete abolition of the chain melting transition (Figure 2, lower right-hand panel). This is not a consequence of the transition shifting to temperatures below 0 °C, as we have seen similar but smaller differences using 2.5 mol % of the NAP-22 peptide. In these samples, the DSC transition was observed with both the cholesterol- and the *ent*-cholesterol-containing samples, but was larger with the cholesterol sample. The difference in the transition behaviour with cholesterol compared with *ent*-cholesterol for this lipid mixture without peptide is negligible (Figure 2, upper curves), whereas in the presence of peptide the differences are dramatic (Figure 2, lower curves). In the case of *N*-acetyl-LWYIK-amide, the DSC results with mixtures containing cholesterol compared with *ent*-cholesterol also show differences suggestive of greater phase separation with cholesterol (Figure 3 and Table 1). In this case, the differences in the DSC data are smaller than those exhibited by the NAP-22 peptide, but they are still significant (Table 1). In addition, there are significant differences in the MAS-NMR spectra with *N*-acetyl-LWYIK-amide in the presence of cholesterol compared with that of *ent*-cholesterol (Figure 5), as discussed in the Results section. The combined observations of DSC and NMR confirm that *N*-acetyl-

LWYIK-amide promotes different membrane arrangements with cholesterol than with *ent*-cholesterol.

In the case of the NAP-22 peptide, the major membrane interaction is through the myristoyl group that has no chirality. However, the presentation of the myristoyl group to the membrane may be affected by the chiral peptide to which it is attached, as well as by membrane insertion of the chiral tyrosine residue. In the case of LWYIK, the chirality of the peptide has only a small effect on the extent of segregation of cholesterol or *ent*-cholesterol (Table 1). There have been several studies on the effect of peptide chirality on the interaction with biological membranes. The biological activity of enantiomers of certain antimicrobial peptides have been shown to be comparable with that of the natural isomer of the peptide [35,36]. The antibacterial activity of a peptide derived from gelsolin that interacts with PtdIns(4,5) $P_2$  is also not affected by peptide chirality [37]. The NAP-22 peptide also interacts with PtdIns(4,5) $P_2$  [38]. In addition, both enantiomers of a peptide that triggers apoptotic cell death and triggers membrane disruption are active [39], as is a neuroactive peptide that inhibits a mechanosensitive channel [40]. In fact, even in cases in which the peptide penetrates into biological membranes and interacts with specific transmembrane helices of integral membrane proteins, there is no requirement for a specific chirality of the peptide [41,42].

The results described above of membrane disruption caused by peptides or peptides to membrane components indicate that they are insensitive to peptide chirality. In contrast, our results indicate that the membrane interactions of the peptides and proteins that are able to induce the formation of cholesterol-rich domains are affected by the small changes in the arrangement and physical properties of the membrane caused by changes in cholesterol chirality [25,26]. As a consequence, the peptide-induced segregation of cholesterol into domains is strongly affected by cholesterol chirality, even though the peptide–lipid interactions that are involved are not very specific.

We would like to acknowledge the assistance of Mr Brian G. Sayer of the Department of Chemistry, McMaster University for assistance in acquiring the NMR spectra. The work was supported by grants from the Canadian Institutes of Health Research (grant MT-7654) and from the U.S. National Institutes of General Medicine (GM-43854).

## REFERENCES

- 1 Simons, K. and Vaz, W. L. C. (2004) Model systems, lipid rafts, and cell membranes. *Annu. Rev. Biophys. Biomol. Struct.* **33**, 269–295
- 2 Epand, R. M. (2004) Do proteins facilitate the formation of cholesterol-rich domains? *Biochim. Biophys. Acta* **1666**, 227–238
- 3 Epand, R. M., Maekawa, S., Yip, C. M. and Epand, R. F. (2001) Protein-induced formation of cholesterol-rich domains. *Biochemistry* **40**, 10514–10521
- 4 Epand, R. M., Sayer, B. G. and Epand, R. F. (2003) Peptide-induced formation of cholesterol-rich domains. *Biochemistry* **42**, 14677–14689
- 5 Frey, D., Laux, T., Xu, L., Schneider, C. and Caroni, P. (2000) Shared and unique roles of CAP23 and GAP43 in actin regulation, neurite outgrowth, and anatomical plasticity. *J. Cell Biol.* **149**, 1443–1454
- 6 Zakharov, V. V., Capony, J. P., Derancourt, J., Kropolova, E. S., Novitskaya, V. A., Bogdanova, M. N. and Mosevitsky, M. I. (2003) Natural N-terminal fragments of brain abundant myristoylated protein BASP1. *Biochim. Biophys. Acta Gen. Subj.* **1622**, 14–19
- 7 Melkonian, K. A., Ostermeyer, A. G., Chen, J. Z., Roth, M. G. and Brown, D. A. (1999) Role of lipid modifications in targeting proteins to detergent-resistant membrane rafts. Many raft proteins are acylated, while few are prenylated. *J. Biol. Chem.* **274**, 3910–3917
- 8 Zacharias, D. A., Violin, J. D., Newton, A. C. and Tsien, R. Y. (2002) Partitioning of lipid-modified monomeric GFPs into membrane microdomains of live cells. *Science* **296**, 913–916
- 9 Epand, R. M., Vuong, P., Yip, C. M., Maekawa, S. and Epand, R. F. (2004) Cholesterol-dependent partitioning of PtdIns(4,5) $P_2$  into membrane domains by the N-terminal fragment of NAP-22 (neuronal axonal myristoylated membrane protein of 22 kDa). *Biochemical J.* **379**, 527–532

- 10 Salzwedel, K., West, J. T. and Hunter, E. (1999) A conserved tryptophan-rich motif in the membrane-proximal region of the human immunodeficiency virus type 1 gp41 ectodomain is important for Env-mediated fusion and virus infectivity. *J. Virol.* **73**, 2469–2480
- 11 Saez-Cirion, A., Nir, S., Lorizate, M., Agirre, A., Cruz, A., Perez-Gil, J. and Nieva, J. L. (2002) Sphingomyelin and cholesterol promote HIV-1 gp41 pretransmembrane sequence surface aggregation and membrane restructuring. *J. Biol. Chem.* **277**, 21776–21785
- 12 Saez-Cirion, A., Arrondo, J. L., Gomara, M. J., Lorizate, M., Iloro, I., Melikyan, G. and Nieva, J. L. (2003) Structural and functional roles of HIV-1 gp41 pretransmembrane sequence segmentation. *Biophys. J.* **85**, 3769–3780
- 13 Li, H., Yao, Z., Degenhardt, B., Teper, G. and Papadopoulos, V. (2001) Cholesterol binding at the cholesterol recognition/interaction amino acid consensus (CRAC) of the peripheral-type benzodiazepine receptor and inhibition of steroidogenesis by an HIV TAT-CRAC peptide. *Proc. Natl. Acad. Sci. U.S.A.* **98**, 1267–1272
- 14 Zhang, W., Crocker, E., McLaughlin, S. and Smith, S. O. (2003) Binding of peptides with basic and aromatic residues to bilayer membranes: phenylalanine in the myristoylated alanine-rich C kinase substrate effector domain penetrates into the hydrophobic core of the bilayer. *J. Biol. Chem.* **278**, 21459–21466
- 15 Rychnovsky, S. D. and Mickus, D. E. (1992) Synthesis of ent-cholesterol, the unnatural enantiomer. *J. Org. Chem.* **57**, 2732–2736
- 16 Sober, H. A. (ed.) (1970) in *Handbook of Biochemistry: Selected Data for Molecular Biology*, p. B75–B76, The Chemical Rubber Co., Cleveland, OH
- 17 Gambhir, A., Hangyas-Mihalayne, G., Zaitseva, I., Cafiso, D. S., Wang, J., Murray, D., Pentyala, S. N., Smith, S. O. and McLaughlin, S. (2004) Electrostatic sequestration of PIP2 on phospholipid membranes by basic/aromatic regions of proteins. *Biophys. J.* **86**, 2188–2207
- 18 Privalov, G., Kavina, V., Freire, E. and Privalov, P. L. (1995) Precise scanning calorimeter for studying thermal properties of biological macromolecules in dilute solution. *Anal. Biochem.* **232**, 79–85
- 19 Forbes, J., Bowers, J., Shan, X., Moran, L., Oldfield, E. and Moscarello, M. A. (1988) Some new developments in solid-state nuclear magnetic resonance spectroscopy studies of lipids and biological membranes, including the effects of cholesterol in model and natural systems. *J. Chem. Soc., Faraday Trans.* **84**, 3821–3849
- 20 Guo, W. and Hamilton, J. A. (1996) <sup>13</sup>C MAS NMR studies of crystalline cholesterol and lipid mixtures modeling atherosclerotic plaques. *Biophys. J.* **71**, 2857–2868
- 21 Arnold, M. R., Kremer, W., Ludemann, H. D. and Kalbitzer, H. R. (2002) <sup>1</sup>H-NMR parameters of common amino acid residues measured in aqueous solutions of the linear tetrapeptides Gly-Gly-X-Ala at pressures between 0.1 and 200 MPa. *Biophys. Chem.* **96**, 129–140
- 22 Wiener, M. C. and White, S. H. (1992) Structure of a fluid dioleoylphosphatidylcholine bilayer determined by joint refinement of x-ray and neutron diffraction data. III. Complete structure. *Biophys. J.* **61**, 437–447
- 23 Feller, S. E., Brown, C. A., Nizza, D. T. and Gawrisch, K. (2002) Nuclear Overhauser enhancement spectroscopy cross-relaxation rates and ethanol distribution across membranes. *Biophys. J.* **82**, 1396–1404
- 24 Pastor, R. W., Venable, R. M. and Feller, S. E. (2002) Lipid bilayers, NMR relaxation, and computer simulations. *Acc. Chem. Res.* **35**, 438–446
- 25 Lalitha, S., Kumar, A. S., Stine, K. J. and Covey, D. F. (2001) Chirality in membranes: first evidence that enantioselective interactions between cholesterol and cell membrane lipids can be a determinant of membrane physical properties. *J. Supramol. Chem.* **1**, 53–61
- 26 Lalitha, S., Kumar, A. S., Stine, K. J. and Covey, D. F. (2001) Enantiospecificity of sterol–lipid interactions: first evidence that the absolute configuration of cholesterol affects the physical properties of cholesterol–sphingomyelin membranes. *Chem. Commun.* 1192–1193
- 27 Westover, E. J., Covey, D. F., Brockman, H. L., Brown, R. E. and Pike, L. J. (2003) Cholesterol depletion results in site-specific increases in epidermal growth factor receptor phosphorylation due to membrane level effects. Studies with cholesterol enantiomers. *J. Biol. Chem.* **278**, 51125–51133
- 28 Westover, E. J. and Covey, D. F. (2004) The enantiomer of cholesterol. *J. Membr. Biol.* **202**, 61–72
- 29 Crowder, C. M., Westover, E. J., Kumar, A. S., Ostlund, Jr, R. E. and Covey, D. F. (2001) Enantiospecificity of cholesterol function *in vivo*. *J. Biol. Chem.* **276**, 44369–44372
- 30 Geva, M., Izhaky, D., Mickus, D. E., Rychnovsky, S. D. and Addadi, L. (2001) Stereoselective recognition of monolayers of cholesterol, ent-cholesterol, and epicholesterol by an antibody. *ChemBioChem.* **2**, 265–271
- 31 Li, Y., Ge, M., Ciani, L., Kuriakose, G., Westover, E. J., Dura, M., Covey, D. F., Freed, J. H., Maxfield, F. R., Lytton, J. and Tabas, I. (2004) Enrichment of endoplasmic reticulum with cholesterol inhibits sarcoplasmic-endoplasmic reticulum calcium ATPase-2b activity in parallel with increased order of membrane lipids: implications for depletion of endoplasmic reticulum calcium stores and apoptosis in cholesterol-loaded macrophages. *J. Biol. Chem.* **279**, 37030–37039
- 32 Zitzer, A., Westover, E. J., Covey, D. F. and Palmer, M. (2003) Differential interaction of the two cholesterol-dependent, membrane-damaging toxins, streptolysin O and *Vibrio cholerae* cytotoxin with enantiomeric cholesterol. *FEBS Lett.* **553**, 229–231
- 33 Richter, R. K., Mickus, D. E., Rychnovsky, S. D. and Molinski, T. F. (2004) Differential modulation of the antifungal activity of amphotericin B by natural and ent-cholesterol. *Bioorg. Med. Chem. Lett.* **14**, 115–118
- 34 Luker, G. D., Pica, C. M., Kumar, A. S., Covey, D. F. and Piwnicka-Worms, D. (2000) Effects of cholesterol and enantiomeric cholesterol on P-glycoprotein localization and function in low-density membrane domains. *Biochemistry* **39**, 7651–7661
- 35 Wade, D., Silberring, J., Soliymani, R., Heikkinen, S., Kilpelainen, I., Lankinen, H. and Kuusela, P. (2000) Antibacterial activities of temporin A analogs. *FEBS Lett.* **479**, 6–9
- 36 Torres-Larios, A., Gurrola, G. B., Zamudio, F. Z. and Possani, L. D. (2000) Hadrurin, a new antimicrobial peptide from the venom of the scorpion *Hadrurus aztecus*. *Eur. J. Biochem.* **267**, 5023–5031
- 37 Bucki, R., Pastore, J. J., Randhawa, P., Vegners, R., Weiner, D. J. and Janmey, P. A. (2004) Antibacterial activities of rhodamine B-conjugated gelsolin-derived peptides compared to those of the antimicrobial peptides cathelicidin LL37, magainin II, and melittin. *Antimicrob. Agents. Chemother.* **48**, 1526–1533
- 38 Epanand, R. F., Sayer, B. G. and Epanand, R. M. (2005) Induction of raft-like domains by a myristoylated NAP-22 peptide and its Tyr mutant. *FEBS J.* **272**, 1792–1803
- 39 Plesniak, L. A., Parducho, J. I., Ziebart, A., Geierstanger, B. H., Whiles, J. A., Melacini, G. and Jennings, P. A. (2004) Orientation and helical conformation of a tissue-specific hunter-killer peptide in micelles. *Protein Sci.* **13**, 1988–1996
- 40 Suchyna, T. M., Tape, S. E., Koeppel, R. E., Andersen, O. S., Sachs, F. and Gottlieb, P. A. (2004) Bilayer-dependent inhibition of mechanosensitive channels by neuroactive peptide enantiomers. *Nature (London)* **430**, 235–240
- 41 Gerber, D., Quintana, F. J., Bloch, I., Cohen, I. R. and Shai, Y. (2005) D-enantiomer peptide of the TCRalpha transmembrane domain inhibits T-cell activation *in vitro* and *in vivo*. *FASEB J.* **19**, 1190–1192
- 42 Sal-Man, N., Gerber, D. and Shai, Y. (2004) Hetero-assembly between all-L- and all-D-amino acid transmembrane domains: forces involved and implication for inactivation of membrane proteins. *J. Mol. Biol.* **344**, 855–864

Received 21 April 2005/27 May 2005; accepted 2 June 2005

Published as BJ Immediate Publication 2 June 2005, doi:10.1042/BJ20050649